

Лук'янченко Юрій Олександрович<sup>1</sup>, кандидат технічних наук, доцент кафедри економічної експертизи та землевпорядкування  
 Гуменний Михайло Іванович<sup>1</sup>, кандидат економічних наук, старший викладач кафедри економічної експертизи та землевпорядкування  
 Лопушанський Олександр Миколайович<sup>1</sup>, кандидат технічних наук, доцент кафедри економічної експертизи та землевпорядкування  
<sup>1</sup>Західноукраїнський національний університет

Lukianchenko Iurii<sup>1</sup>, PhD in Technical Science, Associate Professor of Economic Expertise and Land Management Department, <https://orcid.org/0009-0005-9203-4316>  
 Gumennyi Mykhailo<sup>1</sup>, PhD in Economic Science, lecturer of Economic Expertise and Land Management Department, <https://orcid.org/0000-0002-6704-9656>  
 Lopushanskyi Oleksandr<sup>1</sup>, PhD in Technical Science, Associate Professor of Economic Expertise and Land Management Department, <https://orcid.org/0009-0000-9363-2979>  
<sup>1</sup>West Ukrainian National University

## ВИЗНАЧЕННЯ КООРДИНАТ ПРИЙМАЧА ПІД ЧАС ГНСС ЗМІННЯ З ВИКОРИСТАННЯМ МЕТОДУ НАЙМЕНШИХ КВАДРАТІВ DETERMINATION OF RECEIVER COORDINATES DURING GNSS SURVEYING USING THE LEAST SQUARES METHOD

Лук'янченко Ю. О., Гуменний М. І., Лопушанський О. М.  
 Визначення координат приймача під час ГНСС знімання з використанням методу найменших квадратів.  
 Український журнал прикладної економіки та техніки.  
 2026. Том 11. № 1. С. 227 – 232.

Lukianchenko I., Gumennyi M., Lopushanskyi O.  
 Determination of receiver coordinates during GNSS surveying using the Least Squares method.  
 Ukrainian Journal of Applied Economics and Technology.  
 2026. Volume 11. № 1, pp. 227 – 232.

*The focus of this study is the algorithm for solving the three-dimensional linear inverse resection problem, a fundamental stage in GNSS surveying. The paper also discusses potential factors affecting coordinate determination, including antenna phase center offsets and variations, ephemeris errors, atmospheric effects along the satellite signal propagation path, multipath interference, and other error sources. Global Navigation Satellite Systems (GNSS) form the foundation of modern coordinate reference support. Their applications span an exceptionally wide range in the contemporary world. On the one hand, GNSS technologies have become indispensable tools for mobile device users relying on geolocation services across numerous applications. On the other hand, GNSS serves as a high-precision monitoring system capable of determining global spatial coordinates with sub-millimeter accuracy. Such high-precision applications include monitoring of critical infrastructure (e.g., dams and nuclear power plants), tracking lithospheric plate motion, and observing the effects of seismic activity. Thus, GNSS, deeply integrated into everyday life, ensures the functioning of logistics across maritime, terrestrial, and aerial domains, while serving as the primary coordinate reference framework for most of the engineering and scientific projects. The paper provides a detailed presentation of the mathematical models and computational methodology for receiver coordinate estimation. The study may serve as a theoretical foundation for developing a software module to process satellite observations, particularly for the formulation and solution of normal equations. A numerical example is also presented, demonstrating that approximately five iterations are sufficient to achieve a centimeter-level approximate solution. The results of this work may be useful to engineers and researchers involved in developing software for satellite measurement processing.*

**Keywords:** GNSS surveying, three-dimensional linear inverse resection, least squares method, factors affecting satellite observations.

Основний фокус статті сконцентрований на алгоритмі розв'язання просторової лінійної оберненої засічки, що є одним з основних етапів під час виконання ГНСС знімання. Також в роботі описано можливі фактори, що також впливають на визначення координат: зміщення фазового центру антени, похибки ефемерид, вплив атмосфери, через яку проходить супутниковий сигнал, багатопляховість, та інші. ГНСС - Глобальні Навігаційні Супутникові Системи є основою сучасного координаційного забезпечення. Вони використовуються у дуже широкому спектрі в сучасному світі. З одного боку вони вже стали незамінними супутниками будь-якого користувача мобільного телефону, який використовує геолокацію для безліч різних додатків. В той же час з іншого боку, вони виконують роль системи моніторингу, яка дозволяє визначити просторові глобальні координати із субміліметровою точністю. До таких високоточних задач можна віднести моніторинг критичних інфраструктурних споруд (зрешлі, атомні станції), відстеження руху літосферних плит, спостереження за результатами сейсмічної активності. Отже, можна впевнено сказати, що ГНСС, глибоко інтегрована у повсякденне життя громадян, забезпечує функціонування логістики на морі, на землі та у повітрі, виконує роль основної системи координаційного забезпечення для переважної кількості інженерних та наукових проєктів. В роботі детально наведено математичні залежності та методику обчислення координат приймача. Дана стаття може бути теоретичним підґрунтям для написання програмного модуля для опрацювання супутникових вимірювань, який відповідає за складання та розв'язання нормальних рівнянь. Також в роботі наведено числовий приклад, який показує, що для наближеного розв'язку з точністю на сантиметровому рівні може бути достатньо 5 ітерацій. Робота може бути корисною для інженерів та науковців, які займаються розробленням програмного забезпечення для опрацювання супутникових вимірювань.

**Ключові слова:** ГНСС знімання, просторова лінійна обернена засічка, метод найменших квадратів, чинники, що впливають на супутникові вимірювання.

### Statement of the problem

The primary objective of this study is to formulate detailed mathematical relationships that can be used to develop a software module to construct and solve the normal equations to determine receiver coordinates from measured pseudoranges.

Analysis of recent research and publications. A number of national systems jointly form the Global Navigation Satellite System (GNSS). Traditionally, such systems have been described as consisting of three segments: the space segment, the ground control segment, and the user segment. However, over time, the volume of information required to operate these systems has grown substantially. This includes coordinate time series of permanent reference stations, satellite ephemerides, and various physical models (e.g., tropospheric delay models [1], gravity field models [3, 7], solid Earth tide models [11], among others). It should be emphasized that the number of permanent stations is continuously increasing, new satellites are regularly launched, and more accurate and higher-resolution models are being developed. Moreover, all these datasets are accumulated over time to ensure data continuity and enable long-term analysis.

As a consequence, significant computational resources and data centers are required for storage and processing. The scale of this informational component has become comparable to that of the traditional three segments, leading to an increasingly common view that GNSS should be considered to comprise not three but four segments. This fourth segment may be defined as an infrastructure-information segment, consisting of numerous data centers distributed worldwide that provide the informational backbone of GNSS.

Any satellite navigation system is a large-scale project that requires not only physical infrastructure but also a rigorously formulated mathematical framework for computing corrections to satellite



This is an Open Access article distributed under the terms of the Creative Commons CC-BY 4.0

© Лук'янченко Юрій Олександрович,  
 Гуменний Михайло Іванович,  
 Лопушанський Олександр Миколайович, 2026

observations and directly implementing coordinate estimation algorithms. These tasks are carried out both by national agencies of GNSS-owning states and by private companies developing real-time receiver software.

Nevertheless, the need for software solutions extends beyond real-time positioning. A vast number of permanent ground stations continuously process observational data and generate network solutions (i.e., station coordinates). Another significant application area is the post-processing of satellite observations after the completion of field surveying. Although post-processing requires additional time and computational effort, it can provide superior accuracy. Consequently, GNSS post-processing is widely used by research institutions and in engineering projects that require high-precision coordinate determination.

Post-processing of GNSS data, therefore, represents a complex and essential task. Several leading companies develop specialized software solutions for this purpose. Among the most widely used products are Trimble Business Center, Leica Geo Office, and Topcon Tools [6]. As a rule, these solutions are commercial products, and full functionality requires a license, which is not always feasible for educational institutions training geodetic specialists.

### The purpose of the research

The primary objective of this study is to formulate detailed mathematical relationships that can be used to develop a software module to construct and solve the normal equations to determine receiver coordinates from measured pseudoranges.

### Presentation of the main research material

Let us consider in greater detail the principle of coordinate determination, which is fundamentally based on solving the three-dimensional linear inverse resection problem. In this formulation, the unknown point corresponds to the receiver location at which GNSS observations are performed, while the reference points from which distances to the object are measured are the satellites (Fig. 1), whose coordinates are computed and provided in the form of ephemerides.

However, solving this problem is far from the only challenge that must be addressed to achieve precise coordinate determination from GNSS observations. Some of the most significant factors influencing the accuracy of the final computed coordinates include:

- space segment-related factors;
- environmental factors;
- receiver-related factors.

Let us examine each of these groups of factors in greater detail.

#### Space Segment Factors

Within the space segment, it is generally necessary to account for factors such as antenna phase center offsets, satellite clock asynchrony, and the accuracy of satellite ephemerides. The antenna phase center is a virtual point at which all electromagnetic waves converge; its position is typically calibrated during antenna manufacturing and recorded on the antenna's specification sheet.

The problem of differing time references among satellites is a critical aspect of satellite system operation. GNSS relies on the propagation of electromagnetic waves to determine the distance between a satellite and a receiver. As is well known, the speed of light (in an electromagnetic wave) in a vacuum is constant and equal to 299,792,458 m/s. Therefore, the distance can be calculated from the signal travel time.

However, given such extremely high speeds, highly precise timekeeping is essential for obtaining accurate distance measurements. For example, achieving sub-meter distance accuracy requires time measurements with a precision of approximately 1 nanosecond. The accuracy of GNSS satellite clocks is discussed in detail by B. Männel (2020) [2]. Moreover, certain high-precision applications, such as establishing a national vertical reference system and analyzing the effect of the chosen reference surface, require sub-millimeter coordinate accuracy [4].

To achieve such high temporal precision, satellites are equipped with ultra-precise atomic clocks that track atomic oscillations. The frequency of these oscillations allows time to be measured with extremely high accuracy.

Not all applications require such precision; for example, city-scale navigation typically only requires coordinate accuracy on the order of a few meters. Consequently, satellite coordinates can be determined with varying levels of accuracy. Lower-precision ephemerides can be produced more quickly, while high-precision ephemerides may take up to two weeks to compute, as they require accurate Earth orientation parameters, including polar motion [8, 9]. Considering this, several types of ephemerides with varying levels of accuracy are available, as summarized in Table 1 [5].

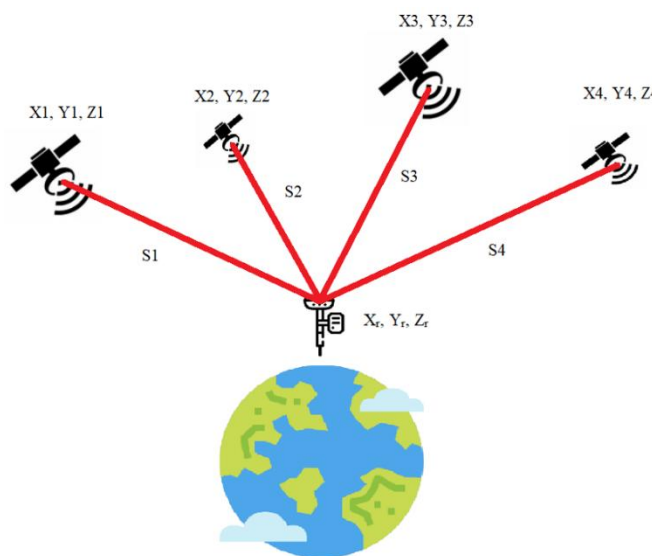


Fig. 1. Configuration of GNSS surveying

Table 1. Types of Ephemerides

type		accuracy	delay	update	Interval
Broadcast	orbit	~ 100 cm	real time	-	1 day
	satellite clock	~ 5 ns, RMS ~ 2.5 ns, SD			
Ultra-rapid (predicted half)	orbits	~ 5 cm	real time	at 03, 09, 15, 21 UTC	15 minutes
	satellite clock	~ 3 ns, RMS ~ 1.5 ns, SD			
Ultra-rapid (observed half)	orbits	~ 3 cm	3 - 9 hours	at 03, 09, 15, 21 UTC	15 minutes
	satellite clock	~ 150 ps, RMS ~ 50 ps, SD			
Rapid	orbits	~ 2.5 cm	17 - 41 hours	at 17 UTC, daily	15 minutes
	satellite clock and station	~ 75 ps, RMS ~ 25 ps, SD			5 minutes
Final	orbits	~ 2.5 cm	12 -19 days	every Friday	15 minutes
	satellite clock and station	~ 75 ps, RMS ~ 25 ps, SD			30 seconds (satellites)

### Environmental Factors

The approximate orbital altitude of navigation satellites is around 20,000 kilometers. This means that, as the signal travels from the satellite to a receiver located on the Earth's surface, the electromagnetic wave passes through various layers of the atmosphere. It is important to note that the speed of light is constant only in a vacuum; when traveling through a medium, its velocity decreases. Two atmospheric layers have the greatest influence on the propagation of electromagnetic waves: the troposphere and the ionosphere.

The ionosphere is a dispersive medium characterized by a high concentration of ions and free electrons. This occurs because the ionosphere, as one of the upper layers of the atmosphere, is among the first to be exposed to solar radiation. As a result, the ionosphere introduces perturbations in the propagation of electromagnetic waves (Fig. 2). To mitigate this effect, dual-frequency GNSS receivers are used. By receiving signals at two different frequencies, it becomes possible to calculate the ionospheric delay and, in effect, almost eliminate the errors caused by it.

As the satellite signal approaches Earth's surface, it passes through the troposphere, where it can be refracted and consequently slowed. This behavior is caused by the inhomogeneous distribution of air masses, particularly the variable water vapor content. Notably, this effect is relatively well understood and can be modeled when the distributions of air masses and water vapor are known. To address this, scientists have developed models of tropospheric delay. Among the most widely used are the Saastamoinen and Hopfield models, which simulate variations in pressure, temperature, and humidity, allowing computation of the signal delay and correction for errors caused by tropospheric propagation.

### Receiver-Related Factors

A wide variety of devices receive GNSS signals, ranging from ordinary smartphones to specialized high-precision dual-frequency receivers. All these devices perform various tasks related to tracking the motion of the objects on which they are installed. It is important to understand that they are also subject to factors that can introduce errors in coordinate determination. The primary factors include antenna phase center offsets and multipath effects. The antenna phase center offset is typically specified during receiver manufacturing and can be corrected using information provided in the receiver's technical documentation. The second factor, multipath effects, occurs when satellite signals reflect off nearby surfaces before reaching the receiver (Fig. 3).

As illustrated in fig. 3, a satellite signal can reach the receiver along multiple paths, reflecting off surrounding objects and the ground. Naturally, the signal that travels along the shortest path is the direct signal, which reaches the receiver without reflection. Based on this principle, signals that are significantly longer than the shortest path can be identified and discarded. This approach can be implemented at the software level to eliminate most signals reflected from nearby objects.

However, software alone does not guarantee sufficient accuracy. Therefore, receiver manufacturers also incorporate physical design features to limit the reception of reflected signals. For example, the lower part of the receiver is often made impermeable to electromagnetic waves to block signals reflected from the ground. Yet this alone is insufficient, as reflected signals can also arrive from above, for instance, after bouncing off trees or nearby buildings. Concentric-ring antennas are used to mitigate this effect, acting as a physical barrier that reduces the impact of multipath reflections.

Therefore, when performing GNSS surveying, it is important to choose open areas with an unobstructed view of the sky to maximize the effectiveness of satellite signal reception.

The three factors discussed above can be considered as directly affecting the measurements. However, the process of coordinating computation involves numerous mathematical operations, during which additional errors can arise from the computational procedures themselves. For instance, satellite coordinates are determined in an inertial reference system, which is not tied to the Earth, whereas receiver coordinates are computed in an Earth-fixed reference frame that rotates with the planet. This necessitates transforming coordinates from one system to another.

Accurate transformation requires information on various phenomena, such as precession, nutation, polar motion, and the Earth's rotation rate. These data enable the conversion from the inertial frame to the Earth-fixed frame. Moreover, each country may have its own national coordinate reference system, requiring further transformations to obtain final coordinates. In the case of Ukraine, for example, it is necessary to convert coordinates to the national coordinate system, UCS2000. An

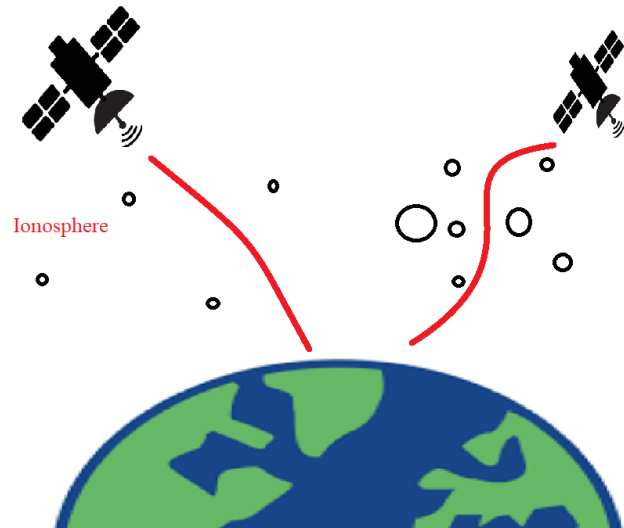


Fig. 2. Influence of the ionosphere on satellite signals

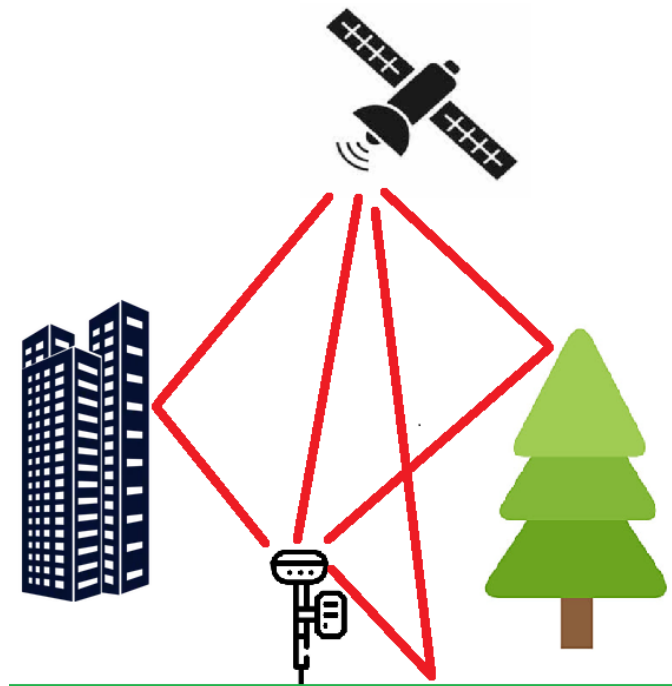


Fig. 3. Influence of multipath effects on GNSS surveying

important step in this process is the transformation from geodetic coordinates to coordinates referenced to the Earth's gravity field, which requires a geoid or quasi-geoid model.

Considering all the above, it is evident that obtaining precise coordinates is a non-trivial task that requires accounting for multiple factors. Nevertheless, one of the most important steps in processing GNSS data is solving the three-dimensional linear inverse resection problem.

### Solution of the three-dimensional linear inverse resection using the Least Squares method

Let us consider a problem that arises in GNSS surveying. Suppose there is a receiver that tracks signals from four satellites. The primary observables are pseudoranges derived from code measurements (the difference between the signal transmission time at the satellite and the signal reception time at the receiver). Let us consider Figure 1, which shows a GNSS receiver with coordinates  $(X_r, Y_r, Z_r)$  and four satellites with coordinates  $(X_1, Y_1, Z_1)$ ,  $(X_2, Y_2, Z_2)$ ,  $(X_3, Y_3, Z_3)$ ,  $(X_4, Y_4, Z_4)$ , respectively. The measured pseudoranges are denoted by  $S_1, S_2, S_3, S_4$ . The unknown parameters are the receiver coordinates, which must be determined from the pseudoranges  $S_i$  and the satellite ephemerides  $X_i, Y_i, Z_i$ . In practice, the number of unknowns is four rather than three. The fourth parameter accounts for the receiver clock offset relative to the satellite clocks. It should be noted that, under real observing conditions, the measured pseudorange is affected by many additional factors. For example, the propagation medium distorts the signal; two principal effects are typically distinguished: the ionospheric delay (which can be mitigated by using a dual-frequency receiver) and the tropospheric delay (which can be modeled using an atmospheric mass distribution model to compute the corresponding signal delay).

Instrument-related errors must also be considered, including antenna phase center offsets and multipath effects. Furthermore, satellites move at high velocities and experience a weaker gravitational field compared to the receiver, which gives rise to relativistic effects. In the present study, we restrict our analysis to the effect of clock asynchrony, which is one of the most significant factors influencing the measured pseudorange.

Thus, our model can be represented by the following equation:

$$S = R + \tau, \quad (1)$$

where,  $S$  – the measured pseudorange,  $R$  – the geometric range between the satellite and the receiver  $\tau$  – correction for receiver-satellite clock asynchrony. The geometric distance from the receiver to the satellite can be computed using the following formula (the satellite index is denoted by  $i$ ):

$$R_i = \sqrt{(X_r - X_i)^2 + (Y_r - Y_i)^2 + (Z_r - Z_i)^2} \quad (2)$$

$$\tau = C \cdot dt, \quad (3)$$

where,  $C$  – speed of light 299 792 458 m/s,  $dt$  – receiver-satellite clock asynchrony (in seconds). Therefore, to solve the four unknowns, at least four observations are needed. The system of equations corresponding to four satellites can be expressed as follows.

$$S_i = \sqrt{(X_r - X_i)^2 + (Y_r - Y_i)^2 + (Z_r - Z_i)^2} + \tau, \quad (4)$$

To solve such a system, we use the Least Squares method. [10]:

$$\mathbf{Ax} + \mathbf{L} = \mathbf{V}, \quad (5)$$

Where,  $\mathbf{A}$  – coefficient matrix of the unknowns,  $\mathbf{x}$  – vector of unknowns,  $\mathbf{L}$  – vector of independent terms,  $\mathbf{V}$  – vector of corrections. It is well known that the vector of unknowns can be determined from the following relation:

$$\mathbf{x} = -(\mathbf{A}^T \mathbf{A})^{-1} (\mathbf{A}^T \mathbf{L}), \quad (6)$$

Examining expression (4), the unknown receiver coordinates  $(X_r, Y_r, Z_r)$  exhibit a nonlinear relationship. In this case, it is necessary to perform linearization. This is done using a well-known approach in mathematics, where the value of a function can be represented based on a known value at a nearby point (the so-called zero-order value of the function) and a small increment, which can be approximated with a certain level of accuracy using the differential of the function. When computing the differential, we will consider only first-order terms.

Thus, we can write the following expression, denoting the approximate receiver coordinates as  $(X_r^0, Y_r^0, Z_r^0)$  and the approximate value of the clock asynchrony correction as  $\tau^0$ .

$$F_i(X_r, Y_r, Z_r, \tau) = F_i(X_r^0, Y_r^0, Z_r^0, \tau^0) + dF_i(X_r^0, Y_r^0, Z_r^0, \tau^0), \quad (7)$$

The differential  $dF$  of a multivariable function can be computed using only the first-order terms.

$$dF = \frac{dF}{dX_r} dX_r + \frac{dF}{dY_r} dY_r + \frac{dF}{dZ_r} dZ_r + \frac{dF}{d\tau} d\tau, \quad (8)$$

Since a differential represents an infinitesimal change, we will replace it with coordinate increments, as we will iteratively determine the final receiver coordinates by progressively computing these increments. More details on this procedure will be provided later.

Thus, we can rewrite equation (8) by replacing the differentials with increments.

$$\Delta F = \frac{dF}{dX_r} \Delta X_r + \frac{dF}{dY_r} \Delta Y_r + \frac{dF}{dZ_r} \Delta Z_r + \frac{dF}{d\tau} \Delta \tau, \quad (9)$$

Now, it is necessary to compute the derivatives  $\frac{dF}{dX_r}, \frac{dF}{dY_r}, \frac{dF}{dZ_r}, \frac{dF}{d\tau}$ . Let us consider equation (4), which represents our measurement model; that is,  $S$  is the function that must be linearized so that all unknowns exhibit a linear relationship

$$F_i(X_r, Y_r, Z_r, \tau) = \sqrt{(X_r - X_i)^2 + (Y_r - Y_i)^2 + (Z_r - Z_i)^2} + \tau, \quad (10)$$

At this point, the partial derivatives can be evaluated

$$\frac{dF_i}{dX_r} = \frac{(X_r - X_i)}{\sqrt{(X_r - X_i)^2 + (Y_r - Y_i)^2 + (Z_r - Z_i)^2}}, \quad (11.1)$$

$$\frac{dF_i}{dY_r} = \frac{(Y_r - Y_i)}{\sqrt{(X_r - X_i)^2 + (Y_r - Y_i)^2 + (Z_r - Z_i)^2}}, \quad (11.2)$$

$$\frac{dF_i}{dZ_r} = \frac{(Z_r - Z_i)}{\sqrt{(X_r - X_i)^2 + (Y_r - Y_i)^2 + (Z_r - Z_i)^2}}, \quad (11.3)$$

$$\frac{dF_i}{d\tau} = 1. \quad (11.4)$$

Considering equation (2), we can now express equation (7) in its linearized form.

$$F_i(X_r, Y_r, Z_r, \tau) = \sqrt{(X_r^0 - X_i)^2 + (Y_r^0 - Y_i)^2 + (Z_r^0 - Z_i)^2} + \tau^0 + \frac{(X_r^0 - X_i)}{\sqrt{(X_r^0 - X_i)^2 + (Y_r^0 - Y_i)^2 + (Z_r^0 - Z_i)^2}} \Delta X_r + \frac{(Y_r^0 - Y_i)}{\sqrt{(X_r^0 - X_i)^2 + (Y_r^0 - Y_i)^2 + (Z_r^0 - Z_i)^2}} \Delta Y_r + \frac{(Z_r^0 - Z_i)}{\sqrt{(X_r^0 - X_i)^2 + (Y_r^0 - Y_i)^2 + (Z_r^0 - Z_i)^2}} \Delta Z_r + \Delta \tau, \quad (12)$$

We can now rewrite equation (4) in linearized form by replacing its right-hand side with the right-hand side of equation (12).

$$S_i = \sqrt{(X_r^0 - X_i)^2 + (Y_r^0 - Y_i)^2 + (Z_r^0 - Z_i)^2} + \tau^0 + \frac{(X_r^0 - X_i)}{\sqrt{(X_r^0 - X_i)^2 + (Y_r^0 - Y_i)^2 + (Z_r^0 - Z_i)^2}} \Delta X_r +$$

$$+ \frac{(Y_r^0 - Y_i)}{\sqrt{(X_r^0 - X_i)^2 + (Y_r^0 - Y_i)^2 + (Z_r^0 - Z_i)^2}} \Delta Y_r + \frac{(Z_r^0 - Z_i)}{\sqrt{(X_r^0 - X_i)^2 + (Y_r^0 - Y_i)^2 + (Z_r^0 - Z_i)^2}} \Delta Z_r + \Delta \tau, \quad (13)$$

By making the substitution  $R_i^0 = \sqrt{(X_r^0 - X_i)^2 + (Y_r^0 - Y_i)^2 + (Z_r^0 - Z_i)^2}$  we rewrite equation (13) in simplified form:

$$S_i = R_i^0 + \tau^0 + \frac{(X_r^0 - X_i)}{R_i^0} \Delta X_r + \frac{(Y_r^0 - Y_i)}{R_i^0} \Delta Y_r + \frac{(Z_r^0 - Z_i)}{R_i^0} \Delta Z_r + \Delta \tau, \quad (14)$$

Once the measurement model  $S_i$  has been linearized, we can proceed to solve for the unknown parameter vector.  $(\Delta X_r, \Delta Y_r, \Delta Z_r, \Delta \tau)$ . Let us rewrite equation (14) in the following form:

$$\frac{(X_r^0 - X_i)}{R_i^0} \Delta X_r + \frac{(Y_r^0 - Y_i)}{R_i^0} \Delta Y_r + \frac{(Z_r^0 - Z_i)}{R_i^0} \Delta Z_r + \Delta \tau + (R_i^0 + \tau^0 - S_i) = 0, \quad (15)$$

Equation (15) would hold true if the measurements were perfectly accurate and the model incorporated all real-world effects affecting the observations. In practice, the right-hand side of equation (15) is therefore nonzero and contains a measurement error, denoted by  $V_i$ . Accounting for these errors, equation (15) can be rewritten in the following form:

$$\frac{(X_r^0 - X_i)}{R_i^0} \Delta X_r + \frac{(Y_r^0 - Y_i)}{R_i^0} \Delta Y_r + \frac{(Z_r^0 - Z_i)}{R_i^0} \Delta Z_r + \Delta \tau + (R_i^0 + \tau^0 - S_i) = V_i. \quad (16)$$

As this equation applies to an arbitrary number of measurements, indexed by  $i$ , the corresponding system of equations can be expressed in matrix form as follows  $Ax + L = V$  (5), where:

$$\begin{pmatrix} \frac{(X_r^0 - X_1)}{R_1^0} & \frac{(Y_r^0 - Y_1)}{R_1^0} & \frac{(Z_r^0 - Z_1)}{R_1^0} & 1 \\ \frac{(X_r^0 - X_2)}{R_2^0} & \frac{(Y_r^0 - Y_2)}{R_2^0} & \frac{(Z_r^0 - Z_2)}{R_2^0} & 1 \\ \dots & \dots & \dots & \dots \\ \frac{(X_r^0 - X_i)}{R_i^0} & \frac{(Y_r^0 - Y_i)}{R_i^0} & \frac{(Z_r^0 - Z_i)}{R_i^0} & 1 \end{pmatrix} - \text{coefficient matrix of the unknowns } A, \quad \begin{pmatrix} \Delta X_r \\ \Delta Y_r \\ \Delta Z_r \\ \Delta \tau \end{pmatrix} - \text{vector of unknowns } x,$$

$$\begin{pmatrix} R_1^0 + \tau^0 - S_1 \\ R_2^0 + \tau^0 - S_2 \\ \dots \\ R_i^0 + \tau^0 - S_i \end{pmatrix} - \text{vector of independent terms } L, \quad \begin{pmatrix} V_1 \\ V_2 \\ \dots \\ V_i \end{pmatrix} - \text{vector of corrections } V.$$

Let  $n$  represent the total number of equations  $n$  ( $i$  - loop index), Then, the matrices and vectors will have the following dimensions:  $A - (n \times 4)$ ,  $x - (4 \times 1)$ ,  $L - (n \times 1)$ ,  $V - (n \times 1)$ .

Therefore, the unknown vector  $x$  is computed according to equation (6). As the parameters were expressed as the sum of their initial approximations and increments, the final values of the unknowns can be determined as follows - formula (17).

In this way, the receiver coordinates  $X_r, Y_r, Z_r$  are obtained, but these values constitute only an initial approximation, as the differentials were replaced by increments and only first-order terms were considered. To achieve higher accuracy, the procedure can be iterated, using the coordinates obtained from the current solution as the new approximations in the next iteration - formula (18),

where, the index  $j$  begins at 1 and denotes the iteration step.

The iteration process may be terminated when the differences between the coordinates from successive iterations fall below a specified threshold. Upon completion of the final iteration, the precision of the estimated parameters can be evaluated using the square roots of the diagonal elements of the covariance matrix - formula (19),

where  $C$  - covariance matrix,  $A^T A$  - normal equation matrix,  $A$  - matrix of coefficients corresponding to the unknown parameters. The covariance matrix is of size  $4 \times 4$ , and the square roots of its diagonal elements  $c_{ii}$  can be employed to obtain a priori assessment of the precision of the estimated parameters.

The following expressions can be employed to compute the a posteriori precision of the estimated parameters - formula (21),

where  $\mu$  - unit weight of the root means square error.

$$\begin{pmatrix} X_r \\ Y_r \\ Z_r \\ \tau \end{pmatrix} = \begin{pmatrix} X_r^0 \\ Y_r^0 \\ Z_r^0 \\ \tau^0 \end{pmatrix} + \begin{pmatrix} \Delta X_r \\ \Delta Y_r \\ \Delta Z_r \\ \Delta \tau \end{pmatrix}, \quad (17) \quad \begin{pmatrix} m_{X_r} \\ m_{Y_r} \\ m_{Z_r} \\ m_{\tau} \end{pmatrix}^{apriory} = \begin{pmatrix} \sqrt{c_{11}} \\ \sqrt{c_{22}} \\ \sqrt{c_{33}} \\ \sqrt{c_{44}} \end{pmatrix}, \quad (20)$$

$$\begin{pmatrix} X_r^j \\ Y_r^j \\ Z_r^j \\ \tau^j \end{pmatrix} = \begin{pmatrix} X_r^{j-1} \\ Y_r^{j-1} \\ Z_r^{j-1} \\ \tau^{j-1} \end{pmatrix} + \begin{pmatrix} \Delta X_r^{j-1} \\ \Delta Y_r^{j-1} \\ \Delta Z_r^{j-1} \\ \Delta \tau^{j-1} \end{pmatrix}, \quad (18) \quad \begin{pmatrix} m_{X_r} \\ m_{Y_r} \\ m_{Z_r} \\ m_{\tau} \end{pmatrix}^{aposterior} = \mu \begin{pmatrix} m_{X_r} \\ m_{Y_r} \\ m_{Z_r} \\ m_{\tau} \end{pmatrix}^{apriory}, \quad (21)$$

$$C = (A^T A)^{-1}, \quad (19) \quad \mu = \sqrt{\frac{\sum_{i=1}^n V_i^2}{n-k}}, \quad (22)$$

$k$  - the required number of observations, which in this case corresponds to the number of unknown parameters, namely 4,  $n$  - the total number of observations.

Let us provide a numerical example. Suppose the initial receiver coordinates are set to zero (for fZaster convergence of the iterative process, approximate coordinates can be used if they are known).

**Table 2. Satellite coordinates and measured pseudoranges.**

	$X_i, m$	$Y_i, m$	$Z_i, m$	$S_i, m$
1	15600000	7540000	20140000	20281272.26
2	-2980000	20350000	11150000	25815332.05
3	-4400000	-9350000	17600000	25817445.03
4	9630000	-9070000	17630000	25037977.53

As can be seen from Table 3, five iterations are sufficient to obtain a stable solution. It is worth noting that synthetic data were used for these calculations. When working with real data, the number of iterations may increase.

### Conclusions and prospects for further research

The input data are presented in table 2.

The iterative process is presented in table 3.

**Table 3. Iterative solutions of the receiver coordinates.**

$j$	$X_r^j$	$Y_r^j$	$Z_r^j$	$\tau^j$
0	0	0	0	0
1	3985568.46	1947587.26	6393145.85	1453235.37
2	3620531.04	1605727.26	4797495.76	52272.50
3	3639246.71	1621474.37	4868492.91	399.01
4	3639200.00	1621400.00	4868099.99	209.86
5	3639200.00	1621400.00	4868100.00	209.86

The paper examines and provides a detailed description of the method for solving the three-dimensional linear inverse resection problem using the least squares method. This stage constitutes the fundamental computational core of all satellite navigation systems, enabling the determination of receiver coordinates. In addition, the study analyzes the factors affecting satellite observations that must be considered during GNSS surveying.

A numerical example demonstrating the implementation of the proposed algorithm is presented. The results show that five iterations are sufficient to achieve sub-centimeter accuracy in the approximate solution. To achieve higher accuracy, the number of iterations should be increased.

Most existing software packages for satellite data processing require paid licenses and cannot be fully utilized in trial versions. For this reason, the present work may be partially useful for institutions involved in geodetic education, as it provides a theoretical basis for developing proprietary software solutions for satellite data processing. Although the inverse resection procedure is described in considerable detail, the information provided is insufficient to develop a complete software system. Therefore, this study should be regarded as the first part of the theoretical and mathematical framework required to create a comprehensive satellite data processing package.

In future research, the authors plan to further develop the theoretical foundations necessary to implement a full-scale software complex for the post-processing of satellite observations.

## Література

1. Dogan A.H., Bahattin E. A new empirical troposphere model using ERA5's monthly average hourly dataset. *Journal of Atmospheric and Solar-Terrestrial Physics*. 2022. Vol. 232. P. 105865. DOI: <https://doi.org/10.1016/j.jastp.2022.105865>.
2. Männel B., Brandt A., Nischan T., Brack A., Sakic P., Bradke M. GFZ rapid product series for the IGS, GFZ Data Services. 2020. DOI: <https://doi.org/10.5880/GFZ.1.1.2020.003>.
3. Foerste C., Bruinsma S.L., Abrikosov O., Lemoine J.-M., Marty J. C., Flechtner F., Balmino G., Barthelmes F., Biancale R. EIGEN-6C4 The latest combined global gravity field model including GOCE data up to degree and order 2190 of GFZ Potsdam and GRGS Toulouse. *GFZ Data Services*. 2014. DOI: <https://doi.org/10.5880/icgem.2015.1>.
4. Lukianchenko I., Lopushanskyi O., Gumennyi M., Chaikivska S. Assessment of gravity and height anomaly changes due to a possible transition of UCS-2000 to the GRS80 ellipsoid. *International Conference of Young Professionals "GeoTerrace-2025"*. 2025. Vol. 2025. P. 1-5. DOI: <https://doi.org/10.3997/2214-4609.202552035>.
5. Johnston G., Riddell A., Hausler G. The International GNSS Service. Springer Handbook of Global Navigation Satellite Systems. Cham, Switzerland: Springer International Publishing. 2017. DOI: <https://doi.org/10.1007/978-3-319-42928-1>.
6. Lukianchenko I.O., Yazlyuk B., Gumennyi M.I., Lopushanskyi O., Kryvoshlyk V.A. Processing of static gnss measurements using trimble business center in the educational process. *The journal Ukrainian Journal of Applied Economics and Technology*. 2025. № 2. P. 395-399. DOI: <https://doi.org/10.36887/2415-8453-2025-2-77>.
7. Lukianchenko I., Gumennyi M., Lopushanskyi O., Semchenko K., Spivak V., Matvyeyev Y. Construction of geoid and quasi-geoid height maps and their comparison on the territory of Europe. *The journal Ukrainian Journal of Applied Economics and Technology*. 2025. № 3. P. 160-165. DOI: <https://doi.org/10.36887/2415-8453-2025-3-31>.
8. Lukianchenko I., Lopushanskyi O., Gumennyi M., Muzyka N., Tartachynska Z. Processing of modern time series of earth's polar motion. *The journal Ukrainian Journal of Applied Economics and Technology*. 2025. № 1. P. 17-2. DOI: <https://doi.org/10.36887/2415-8453-2025-1-2>.
9. Lukianchenko I., Lopushanskyi O., Gumennyi M., Perovych I.L., Lopushanska M. Earth's modern polar motion analysis theoretical aspects. *The journal Ukrainian Journal of Applied Economics and Technology*. 2024. № 3. P. 308-311. DOI: <https://doi.org/10.36887/2415-8453-2024-3-54>.
10. Marjetič A., Ambrožič T., Savšek S. Use of Total Least Squares Adjustment in Geodetic Applications. *Applied Sciences*. 2024. № 14(6). P. 2516. DOI: <https://doi.org/10.3390/app14062516>.
11. Xiaoqing X., Haidong P., Fei T., Guohong F., Zexun W. A comparison of global and regional ocean tide models with tide gauges in the East Asian marginal seas. *Journal of Sea Research*. 2024. Vol. 201. P. 102527. DOI: <https://doi.org/10.1016/j.seares.2024.102527>.

## References

1. Dogan, A.H., Bahattin, E. (2022). «A new empirical troposphere model using ERA5's monthly average hourly dataset». *Journal of Atmospheric and Solar-Terrestrial Physics*. Vol. 232. pp. 105865. DOI: <https://doi.org/10.1016/j.jastp.2022.105865>.
2. Männel, B., Brandt, A., Nischan, T., Brack, A., Sakic, P., Bradke, M. (2020). GFZ rapid product series for the IGS. GFZ Data Services. DOI: <https://doi.org/10.5880/GFZ.1.1.2020.003>.
3. Foerste, C., Bruinsma, S.L., Abrikosov, O., Lemoine, J.-M., Marty, J. C., Flechtner, F., Balmino, G., Barthelmes, F., Biancale, R. (2014). EIGEN-6C4 The latest combined global gravity field model including GOCE data up to degree and order 2190 of GFZ Potsdam and GRGS Toulouse. GFZ Data Services. DOI: <https://doi.org/10.5880/icgem.2015.1>.
4. Lukianchenko, I., Lopushanskyi, O., Gumennyi, M., Chaikivska, S. (2025). «Assessment of gravity and height anomaly changes due to a possible transition of UCS-2000 to the GRS80 ellipsoid». *International Conference of Young Professionals "GeoTerrace-2025"*. Vol. 2025. pp. 1-5. DOI: <https://doi.org/10.3997/2214-4609.202552035>.
5. Johnston, G., Riddell, A., Hausler, G. (2017). The International GNSS Service. Teunissen, Springer Handbook of Global Navigation Satellite Systems. Cham, Switzerland: Springer International Publishing. DOI: <https://doi.org/10.1007/978-3-319-42928-1>.
6. Lukianchenko, I.O., Yazlyuk, B., Gumennyi, M.I., Lopushanskyi, O., Kryvoshlyk, V.A. (2025). «Processing of static gnss measurements using trimble business center in the educational process». *The journal Ukrainian Journal of Applied Economics and Technology*. № 2. pp. 395-399. DOI: <https://doi.org/10.36887/2415-8453-2025-2-77>.
7. Lukianchenko, I., Gumennyi, M., Lopushanskyi, O., Semchenko, K., Spivak, V., Matvyeyev, Y. (2025). «Construction of geoid and quasi-geoid height maps and their comparison on the territory of Europe». *The journal Ukrainian Journal of Applied Economics and Technology*. № 3. pp. 160-165. DOI: <https://doi.org/10.36887/2415-8453-2025-3-31>.
8. Lukianchenko, I., Lopushanskyi, O., Gumennyi, M., Muzyka, N., Tartachynska, Z. (2025). «Processing of modern time series of earth's polar motion». *The journal Ukrainian Journal of Applied Economics and Technology*. № 1. pp. 17-2. DOI: <https://doi.org/10.36887/2415-8453-2025-1-2>.
9. Lukianchenko, I., Lopushanskyi, O., Gumennyi, M., Perovych, I.L., Lopushanska, M. (2024). «Earth's modern polar motion analysis theoretical aspects». *The journal Ukrainian Journal of Applied Economics and Technology*. № 3. pp. 308-311. DOI: <https://doi.org/10.36887/2415-8453-2024-3-54>.
10. Marjetič, A., Ambrožič, T., Savšek, S. (2024). «Use of Total Least Squares Adjustment in Geodetic Applications». *Applied Sciences*. № 14(6). pp. 2516. DOI: <https://doi.org/10.3390/app14062516>.
11. Xiaoqing, X., Haidong, P., Fei, T., Guohong, F., Zexun, W. (2024). «A comparison of global and regional ocean tide models with tide gauges in the East Asian marginal seas». *Journal of Sea Research*. Vol. 201. pp. 102527. DOI: <https://doi.org/10.1016/j.seares.2024.102527>.

Стаття надійшла до редакції / Received 10.02.2026  
Опубліковано / Published 25.02.2026

Прийнята до друку / Accepted 18.02.2026